

# NON-LINEAR CHARACTERISATION OF PIEZOELECTRIC AND ELECTROSTRICTIVE CERAMICS AND SINGLE CRYSTALS

Binu Mukherjee – Royal Military College of Canada

## Introduction

Piezoelectric and electrostrictive materials are important constituents of electromechanical sensors, actuators and smart structures. Piezoelectric materials produce a strain,  $S$ , under the influence of an external electric field,  $E$ , or become electrically polarised under the influence of an external stress,  $T$ . The property of piezoelectricity is closely related to the phenomenon of ferroelectricity, which describes the spontaneous polarisation in a crystal that can be changed between two or more distinct directions with respect to the crystal axes through the application of an external electric field. This ability of ferroelectric materials to switch polarisation under an external electric field from a random orientation to a preferred direction is used in a variety of polycrystalline ferroelectric ceramics to produce a polycrystalline piezoelectric ceramic with a preferred direction of net polarisation. This process is known as “poling”. In an unpoled ceramic the individual domains in the ceramic have randomly oriented directions of polarisation so that the ceramic as a whole shows little or no polarisation. The partial alignment of domains during poling creates a net spontaneous polarisation in the poling direction and the ceramic shows a  $C_{\infty}$  symmetry around that direction.

Piezoelectricity can be mathematically derived from a phenomenological model derived from thermodynamical potentials. The derivations are not unique and the set of equations describing the direct and converse piezoelectric effect depend on the choice of potential and the independent variables used.<sup>1,2</sup> For example, one set of such linear constitutive relations is

$$S_p = s_{pq}^E T_q + d_{mp} E_m \quad \text{and} \quad D_m = \varepsilon_{mn}^T E_n + d_{mp} T_p, \quad (1)$$

where  $D$  is the electric displacement,  $s$  is the elastic compliance,  $d$  is the piezoelectric constant and  $\varepsilon$  is the dielectric permittivity. The superscripts of the constants designate the independent variable that is held constant when defining the material coefficient and the subscripts define directions that take account of the anisotropic nature of the material. It has been shown that the piezoelectric constant  $d_{mp}$  that occurs in the two equations is the same.<sup>3</sup> The material constants form a  $9 \times 9$  matrix with 1, 2, 3 designating the orthonormal directions and 4, 5, 6 designating the shear directions. For the commonly used piezoelectric ceramics with  $C_{\infty}$  symmetry, such as lead zirconate titanate or PZT, there are ten non-zero, independent matrix elements consisting of 5 independent elastic coefficients ( $s_{11}^E, s_{12}^E, s_{13}^E, s_{33}^E, s_{55}^E$ ), 3 independent piezoelectric coefficients ( $d_{31}, d_{15}, d_{33}$ ) and 2 independent dielectric constants ( $\varepsilon_{11}^T, \varepsilon_{33}^T$ ).<sup>4</sup> While the linear constitutive relations can be written in ways other than that shown in (1), there are only 10 independent constants. The full, reduced, matrix for these materials can be found in the IEEE standard<sup>4</sup>, which also contains the equations that allow one to convert from one set of constitutive equations/matrix to another.

Ideally, under small fields and stresses and for materials with low losses within a limited frequency range, these 10 constants contain all the information required to predict the behaviour of the material when a stress, strain or electric field is applied to it. However, the continuing need for large actuation and a continually increasing variety of applications has seen the use of piezoelectric materials under a growing range of conditions. These include the application of large fields and stresses as well as a wider range of frequencies and temperatures. In practice most piezoelectric

materials display dispersion and non-linearities, have measurable losses and their properties are temperature dependent. The last two decades has also seen the development of finite element packages to model piezoelectric materials, such as PZFlex<sup>5</sup>, and some of these are sufficiently precise so as to require very accurate material constants. All of the above has pointed to the need for better characterisation of piezoelectric materials: both for the traditional ceramics and polymers as well as for the new high strain single crystals in the lead zinc niobate – lead titanate and lead magnesium niobate – lead titanate families. The Laboratory for Ferroelectric Materials at the Royal Military College of Canada has a continuing programme for improving the characterisation of these materials and this paper presents a summary of the work of this group since its establishment in 1988. Fuller details regarding the work can be obtained from the references mentioned in the paper.

### **Impedance Spectroscopy or Resonance Methods**

The most widely used technique for determining all the 10 relevant constants for piezoelectric ceramics is the resonance technique outlined in the IEEE standard on piezoelectricity.<sup>4</sup> A piezoelectric sample of specific geometry is excited with an AC signal and an impedance analyser is used to determine the complex impedance and admittance as a function of frequency. The impedance spectra contain resonances that result from ultrasonic standing waves in the material. Several particular frequencies may be defined from these spectra: the parallel resonance frequency,  $f_p$ , is the frequency at which the resistance  $R$  is a maximum, the sideband frequencies,  $f_{+1/2}$  and  $f_{-1/2}$ , correspond to the maximum and minimum in the reactance  $X$ , the series resonance frequency  $f_s$  is the frequency at which the conductance  $G$  is a maximum and the sideband frequencies,  $f_{+1/2s}$  and  $f_{-1/2s}$ , correspond to the maximum and minimum of the susceptance  $B$ . Five resonance modes are commonly used to find the full set of material coefficients for a piezoelectric ceramic and each mode requires samples with specific aspect ratios<sup>4</sup> to ensure that the sample is excited in a mode where the one-dimensional approximation is valid and coupling between the modes is invalid. It should be noted that the aspect ratios may be relaxed for materials with low mechanical  $Q$  whereas they need to be more stringent for materials with a high mechanical  $Q$  and high electromechanical coupling. The impedance equations that govern the various resonance spectra have been derived from the phenomenological theory of piezoelectricity<sup>6,7</sup> for the case of real material constants assuming lossless materials. These equations express the impedance as a function of the appropriate material constants and of the particular frequencies mentioned above. Holland<sup>8</sup> suggested that the losses in a piezoelectric material may be taken into account by representing the material constants as complex coefficients. Sherrit<sup>9</sup> has re-derived the impedance equations for the various resonance geometries using complex material constants so as to include the dielectric, mechanical and piezoelectric losses in the material. The complex material constants can be found by comparing the impedance equations with the appropriate experimental impedance curve around the fundamental resonance and finding the best fit. Numerous techniques have been proposed for this purpose<sup>10,11,12,13,14,15,16</sup>, including some that have been developed in our laboratory. Some of the advantages and disadvantages of the various techniques have been discussed by Mukherjee and Sherrit<sup>17</sup>, by Kwok et al<sup>18</sup> and by Pardo.<sup>19</sup> Commercial software is now available for carrying out the analysis of the experimental resonance curves.<sup>20</sup> The physical significance of the complex material constants has been discussed by Mukherjee and Sherrit<sup>21</sup> and a discussion may also be found on the PRAP website.<sup>20</sup> An example of a complete characterisation is shown in Table 1<sup>22</sup> and it shows the full set of measured and calculated complex material constants for the Motorola 3203HD piezoceramic. The table shows that some redundancy is built in to the method, as the same coefficient may be determined from more than one resonance measurement. These may be used to find an average value but it should be noted that the measurements are not all at the same frequency and in the presence of significant dispersion it is important to take note of the frequency at

which the constant has been determined. A more detailed understanding of dispersion in a piezoceramic can be obtained by carrying out the resonance analysis at the fundamental resonance and at higher order resonances.<sup>22</sup> While the dispersion in piezoceramics is not normally very significant, it becomes important in some other piezoelectric materials, as for example in polyvinylidene fluoride - tetrafluoroethylene copolymers, and in such cases the real and complex parts of the material constants may be expressed as polynomials in frequency<sup>23</sup> and the applications engineer can then calculate the value of the constant at the frequency of interest.

TABLE 1: The reduced matrix of Motorola 3203HD PZT ceramic including the electromechanical coupling determined at fundamental resonance of each mode<sup>22</sup>. The values shown are averages over 4 specimens and the spread of values is indicated by the standard deviations over the 4 specimens.

Material Constant	Mode	Frequency kHz	Value		Standard deviation %	
			Real	Imaginary	Real	Imaginary
$s_{11}^E$ (m <sup>2</sup> /N) x 10 <sup>11</sup>	LTE	71.5	1.56	-0.030	0.63	5.2
$s_{11}^E$ (m <sup>2</sup> /N) x 10 <sup>11</sup>	RAD	150.9	1.55	-0.032	0.45	2.8
$s_{11}^E$ (m <sup>2</sup> /N) x 10 <sup>11</sup>	Average		1.56	-0.031		
$s_{12}^E$ (m <sup>2</sup> /N) x 10 <sup>11</sup>	RAD	150.9	-0.420	0.012	3.9	4.9
$s_{13}^E$ (m <sup>2</sup> /N) x 10 <sup>11</sup>	Calculated	Smits'formula	-0.821	0.034	N/A	N/A
$s_{33}^E$ (m <sup>2</sup> /N) x 10 <sup>11</sup>	LE	199	1.89	-0.034	1.0	0.78
$s_{55}^E$ (m <sup>2</sup> /N) x 10 <sup>11</sup>	TS	2730	3.92	-0.13	2.9	4.3
$s_{66}^E$ (m <sup>2</sup> /N) x 10 <sup>11</sup>	Calculated	IEEE formula	3.96	-0.086	N/A	N/A
$c_{33}^D$ (m <sup>2</sup> /N) x 10 <sup>11</sup>	TE	6390	1.77	0.023	2.0	11
$d_{31}$ (C/N) x 10 <sup>-12</sup>	LTE	71.5	-297	9.7	0.7	7.1
$d_{31}$ (C/N) x 10 <sup>-12</sup>	RAD	150.9	-293	10	0.68	5.8
$d_{31}$ (C/N) x 10 <sup>-12</sup>	Average		-295	9.9		
$d_{33}$ (C/N) x 10 <sup>-12</sup>	LE	199	564	-15	3.1	17
$d_{15}$ (C/N) x 10 <sup>-12</sup>	TS	2730	560	-30	4.6	11
$\epsilon_{11}^T$ (F/m) x 10 <sup>-8</sup>	TS	2730	2.14	-0.13	0.44	6.8
$\epsilon_{33}^T$ (F/m) x 10 <sup>-8</sup>	RAD	150.9	3.06	-0.11	1.1	6.5
$\epsilon_{33}^T$ (F/m) x 10 <sup>-8</sup>	LT	71.5	2.83	-0.061	1.9	9.4
$\epsilon_{33}^T$ (F/m) x 10 <sup>-8</sup>	Average		2.95	-0.083		
$\epsilon_{33}^S$ (F/m) x 10 <sup>-8</sup>	TE	6390	1.06	-0.053	2.0	4.2
$k_{33}$	LE	199	0.763	-0.0029	0.52	45
$k_{31}$	LTE	71.5	0.447	-0.0054	0.90	16
$k_{15}$	TS	2730	0.611	-0.0034	3.1	37
$k_p$	RAD	150.9	0.706	-0.0062	0.45	6.1
$k_t$	TE	6390	0.536	-0.0050	0.46	12

## Equivalent Circuits

In designing devices it is sometimes useful to have an equivalent electrical circuit to represent the material. The most commonly used equivalent circuit to represent a piezoelectric vibrator has been the Van Dyke circuit, which uses four real circuit parameters. Sherrit et al have shown that the Van Dyke circuit cannot take account of all the losses in the piezoelectric material and they have proposed an alternative model<sup>24,25</sup> with three complex circuit parameters for each resonator geometry; the circuit parameters can be calculated from the material constants and vice versa.

## Temperature Dependence of the Material Constants

The resonance experiments outlined above have been carried out with the ceramic samples placed in a Thermotron programmable temperature chamber that allows the temperature to be controlled between  $-72^{\circ}\text{C}$  and  $174^{\circ}\text{C}$ . The variation of the dielectric, elastic and piezoelectric constants as a function of temperature have been measured for the hard EC-69 and soft EC-76 ceramics made by Edo Ceramics Inc.<sup>26</sup> Here, in Fig. 1, we only show the variation of the piezoelectric constants of the two types of ceramic as a function of temperature.

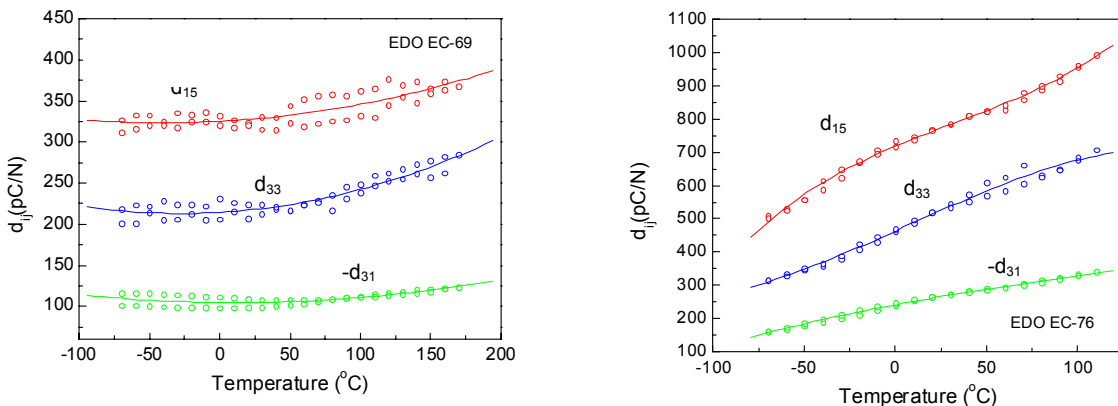


Figure 1: Temperature dependence of the piezoelectric constants of EDO EC-69 and EC-76 ceramics.

## Electric Field Dependence of the Piezoelectric Response

Although equation (1) suggests that the piezoelectric strain is a linear function of the applied field, this is only true when small fields are applied. As larger electric fields are applied in an effort to obtain larger strains, the response of the ceramic becomes non-linear. The phenomenological equations (1) can be uncoupled thereby allowing the strain and dielectric displacement to be monitored as a function of electric field, which facilitates the determination of the piezoelectric coefficients.<sup>27</sup>

The variation of the piezoelectric constant  $d$  and the permittivity  $\epsilon$  as a function of the applied electric field can be studied under two different experimental conditions: (a) quasistatic experiments that give the value of the constants under near DC conditions, and (b) resonance experiments that provide the material constants at the appropriate resonance frequency. The difference in the significance of these two types of experiments can be understood with reference to Fig. 2. The main curve in the figure shows a typical curve that is obtained when a varying electric field, below the

coercive field, is applied to a piezoelectric material, and the resultant strain is measured. A measurable hysteresis is caused by irreversible domain wall motions that are characteristic of ferroelectric materials. Zhang et al<sup>28</sup> studied the onset of irreversibility in such materials and found that each material had a plateau region where the permittivity and the piezoelectric constant were independent of field and they attributed this field independence to reversible domain motions that characterise the intrinsic piezoelectric response. Under the application of a large electric field, the domain walls move to maintain a minimum in the domain energy and the some of the domains engulf other domains or change shape irreversibly, which contributes to the net strain and polarisation and constitutes the extrinsic piezoelectric response. The total piezoelectric response is the sum of the reversible and irreversible contributions. Figure 2 shows that the slopes of the two types of measurement are different and therefore the material constants found from these measurements cannot be the same. When a large low-frequency electric or stress field is applied and the corresponding hysteresis loop is measured, an average value of the dielectric or piezoelectric constant can be found from the average slope of the hysteresis curve. However, when a large DC electric or stress field is applied and a small AC field is used to measure the response under that DC field the slope of the AC response can be said to provide a dynamic value of the constant. This discussion underlines the importance of determining material constants under conditions appropriate for any particular application.

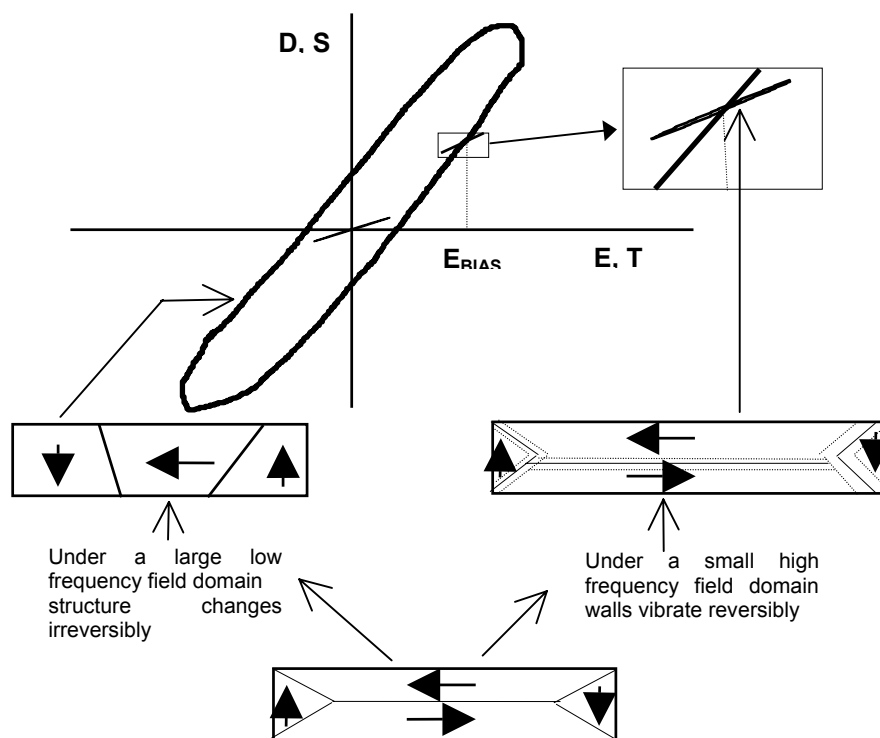


Figure 2: The relationship between the reversible and irreversible domain motion and the resultant strain S or electric displacement D as a function of applied stress T or electric field E.

As will be clear from the above discussion, when small electric or stress fields are applied to a piezoceramic, no hysteresis is observed and a well defined slope yields values of either the piezoelectric constant or the permittivity resulting from intrinsic contributions. As the electric field is increased, domain effects begin to occur, producing some hysteresis and the average slope increases as both intrinsic and extrinsic effects contribute to the piezoelectric and dielectric responses<sup>29</sup>. Such an average slope and average values of the material constants can only be

defined when the hysteresis is not too pronounced and we have found that, in this regime, the average values of the piezoelectric and dielectric constants increase linearly with applied electric field.<sup>29</sup>

### Strain response under large applied electric fields

When very high fields are applied and significant hysteresis is present, it becomes difficult to define an average slope. However the total strain/displacement can be measured as a function of applied electric field/stress and their ratio can be used to define an effective average material coefficient. Alternatively a large DC bias field may be applied and a small AC field can be used to find the response and to define a dynamic constant. The determination of the piezoelectric response under these conditions requires direct measurement of the strain. In our laboratory we have different experimental methods of measuring strains including the relatively simple optical lever<sup>30</sup>, the differential variable reluctance transducer (DVRT) and laser Doppler interferometry. The latter is the most versatile of the direct strain measuring instruments as it allows the measurement of AC strains.<sup>31</sup> Our measurement system uses a Zygo ZMI 2000 heterodyne laser Doppler interferometer<sup>32</sup> with a resolution of 0.62 nm and it has been described elsewhere.<sup>33</sup> The system may be used to directly measure linear strains as well as shear strains<sup>33</sup> and thus it allows us to determine all the piezoelectric  $d$  coefficients. Figure 3 shows the variation of the average values of the  $d_{33}$ ,  $d_{31}$  and  $d_{15}$  as a function of applied electric fields up to about 1 MV/m for two types of lead zirconate titanate (PZT) ceramics: the fairly soft EC-65 and the hard EC-69 ceramics made by EDO Ceramics Inc. Soft PZT is characterised by a high piezoelectric constant and mobile domain boundaries<sup>34</sup> so that extrinsic contributions are inherently more important and their effect is increased at higher fields.<sup>35</sup> The observed increase in the  $d$  coefficients in the soft PZT, EC-65, is likely due to the larger extrinsic contribution resulting from increased domain switching under the influence of large fields. The nonlinearities observed are stronger than what would be predicted by the Rayleigh law as can be seen from the following polynomial fits to the curves for the EC-65 PZT:

$$\begin{aligned}d_{15} &= 560 + 1170E - 205E^2 + 142E^3, \\d_{33} &= 455 + 529E - 153E^2 + 43E^3, \\d_{31} &= -192 - 312E + 126E^2 - 12E^3.\end{aligned}$$

Although Fig. 3 does not show any significant non-linearity in the  $d$  coefficients of the hard EC-69 ceramic, this is only because the applied fields here were not high enough, as will be seen later, in Fig. 5. The acceptor doped hard PZT suppresses domain wall response so that higher fields are required for the same effects to be observed.

### Strain response under the application of a DC bias field

Our laser Doppler interferometer system has also been used to study the DC bias dependence of the piezoelectric strain. Figure 4 shows the DC field dependence of the dynamic  $d_{33}$  for both types of piezoceramics at various frequencies. When a positive DC bias is applied to the well poled hard PZT, EC-69, a very small decrease in  $d_{33}$  is observed. However, when a negative DC bias is applied to this ceramic, the  $d_{33}$  increases significantly as a function of the bias field. For a well-poled ceramic, the bias field does not significantly increase the poling but rather helps to pin the domains leading to the observed small decrease in  $d_{33}$ . However, a negative bias causes de-pinning (de-ageing)<sup>36</sup> of the domain walls and this increases the extrinsic contribution to the piezoelectric strain and leads to higher values of  $d_{33}$ . In the case of the soft PZT, EC-65, a negative bias field initially causes a rise in the  $d_{33}$  due to similar de-pinning effects. However the soft PZT has low values of

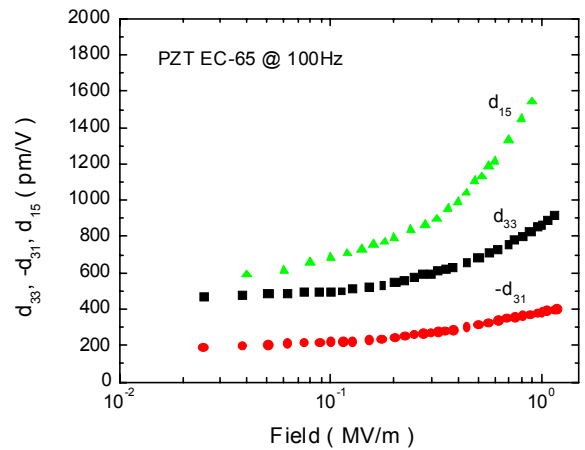
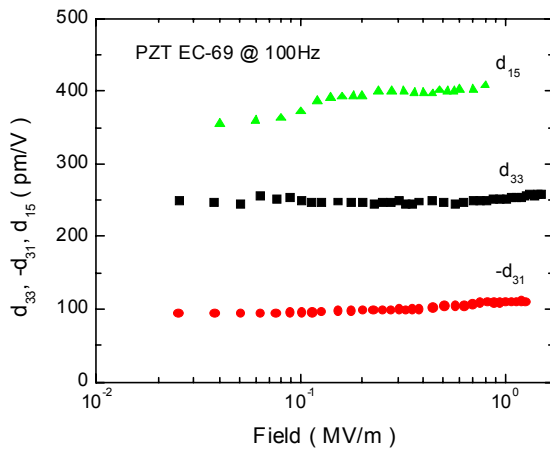


Figure 3: Piezoelectric  $d$  coefficients of hard EC-69 and soft EC-65 PZT ceramics as a function of an applied 100 Hz AC electric field.

the coercive fields and when the negative fields reach this value the PZT depoles causing a sharp drop in the  $d_{33}$ . If the negative field is further increased the material now re-poles in the direction of the applied field, which now becomes a positive bias and contributes to domain pinning that reduces the  $d_{33}$ . Since extrinsic effects contribute more to the strain in soft PZT, these effects are seen to be larger in the case of the soft PZT.

Figure 5 shows the AC measuring field dependence of the dynamic  $d_{33}$  in the presence of various positive DC bias field levels. This figure shows measurements made up to AC fields of 5 MV/m. The hard EC-69 ceramic shows little dependence on the AC field or the DC bias field up to 1 MV/m. However for higher AC fields the material shows a significant non-linear increase in  $d_{33}$  caused by the

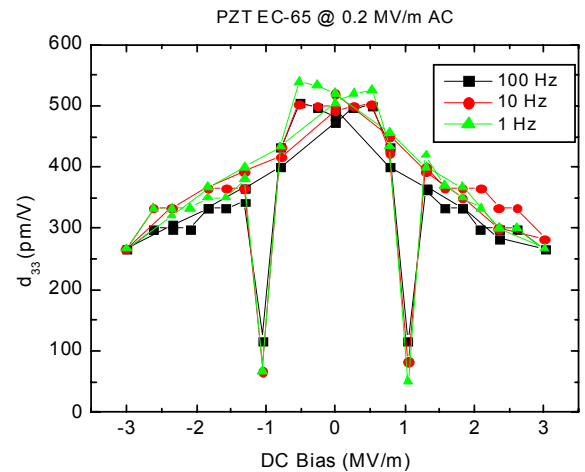
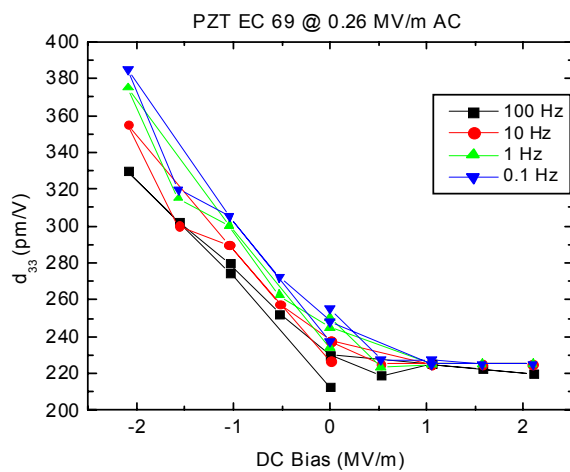


Figure 4: DC bias field dependence of the two types of PZT at various frequencies.

de-ageing and depoling processes that increase the extrinsic domain contributions but the non-linear increase is suppressed by the application of a positive DC bias, which stabilises the domain structure and inhibits de-ageing. In the case of the soft PZT, EC-65, also the non-linear response is seen to be suppressed by DC bias fields. The general result that a DC bias reduces the non-linear response in a piezoceramic is in agreement with earlier observations by Masuda and Baba.<sup>37</sup>

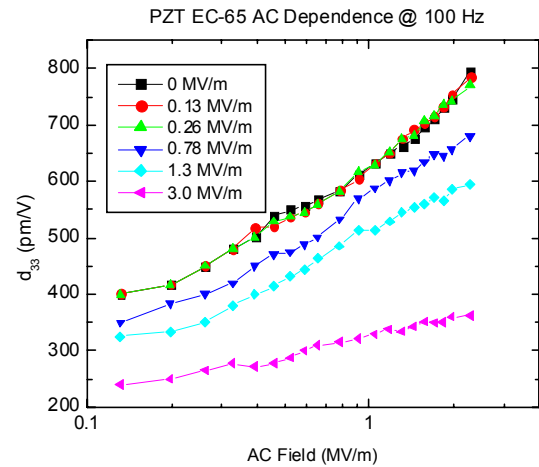
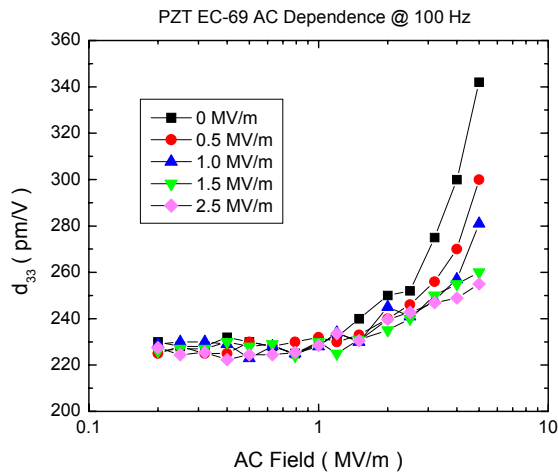


Figure 5: AC field dependence of the  $d_{33}$  for the two types of PZT under positive DC bias fields (in the same direction as the poling).

### High frequency properties under DC Bias

The methods of impedance analysis of piezoelectric resonators described earlier have been used to study the radial mode resonance of three types of PZT samples, EC-69, EC-65 and the very soft EC-76, when the samples were placed under DC bias fields that ranged up to  $\pm 3$  kV. PRAP software<sup>20</sup> was used to analyse the impedance curves and find the values of the elastic compliances  $s_{11}^E$  and  $s_{12}^E$ , the dielectric constant  $\epsilon_{33}^T$ , the piezoelectric constant  $d_{31}$  and the planar electromechanical coupling constant  $k_p$ , all as a function of the DC bias field. Our results are shown in Fig. 6. It should be noted that the EC-76 ceramic is so soft that no meaningful measurements could be made with negative DC fields as very small negative fields were sufficient to depole these ceramics. The EC-65 ceramic depoled at negative fields of about  $-0.8$  MV/m. The hard PZT, EC-69 showed no depoling up to the maximum DC fields applied. Similarly to what was observed in our low frequency interferometric measurements, the piezoelectric constant  $d_{31}$  decreases when a positive DC bias is applied to the specimen and it increases when a negative bias field is applied until depoling occurs. The constants  $s_{11}^E$ ,  $\epsilon_{33}^T$  and  $k_p$  also showed a similar behaviour. However, the elastic compliance  $s_{12}^E$  increased with the application of a positive DC bias and decreased with a negative bias before depoling occurred.

In summary, it can be said that a DC bias in the poling direction clamps the domains and reduces the strain. However as the AC field is increased the strain increases due to depinning and depoling effects. On the other hand a negative DC bias causes field-induced de-ageing (unclamping of domain walls) that results in an increase in the piezoelectric constant, the dielectric constant and the electromechanical coupling constant. Fuller details of our measurements are available elsewhere.<sup>33</sup>

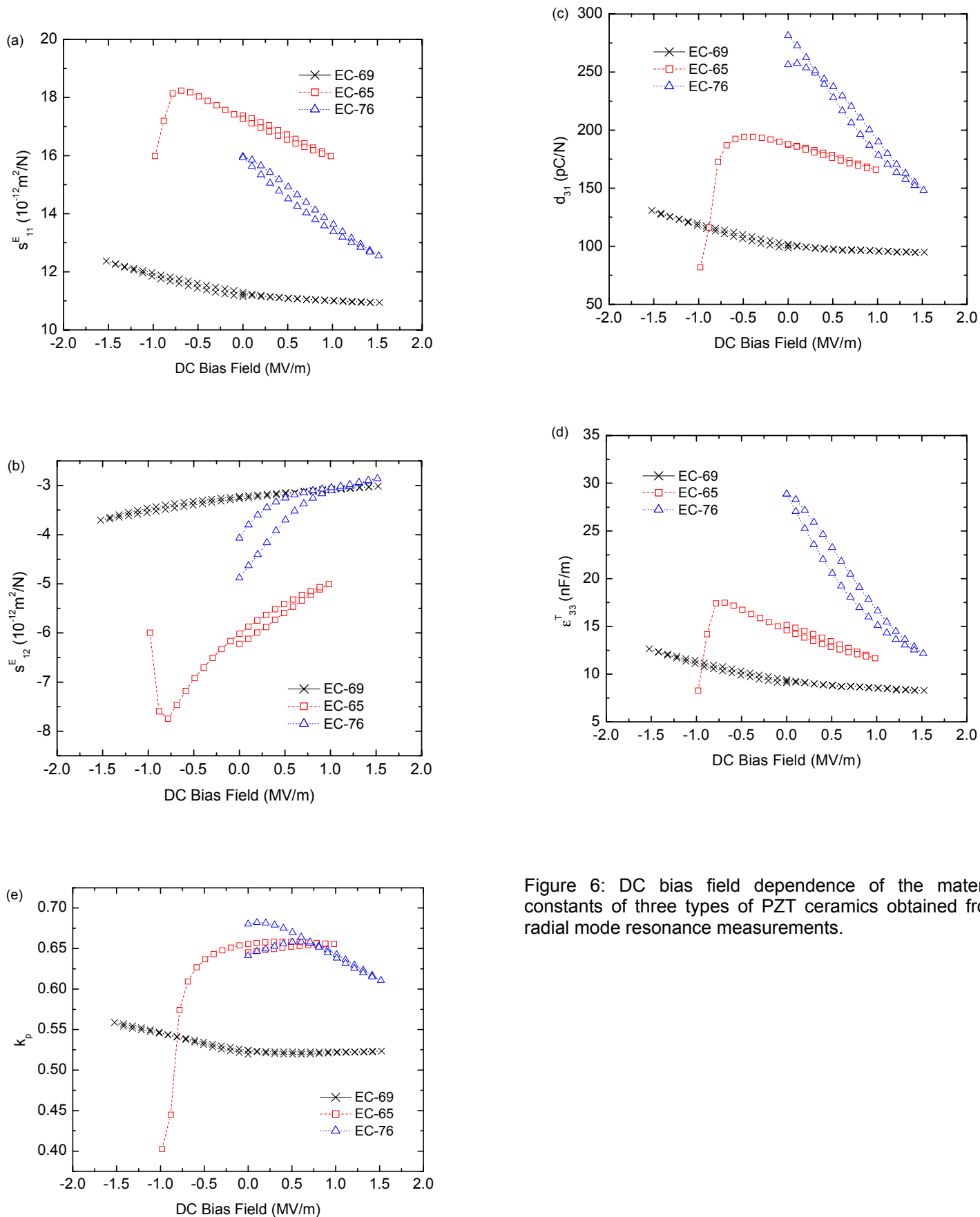


Figure 6: DC bias field dependence of the material constants of three types of PZT ceramics obtained from radial mode resonance measurements.

## Stress Dependence of the Piezoelectric Response

It has been shown that mechanical stress can cause re-orientation of polarisation and depoling in piezoelectric ceramics.<sup>38,39,40</sup> Equation (1) shows that if the electric field is kept constant or is set to zero (short circuit condition), the dielectric displacement and the strain can be measured and the piezoelectric, dielectric and elastic constants can be determined as a function of stress.<sup>27,41</sup> Our measurements were carried out on the soft EC-65 and the EC-69 ceramics mentioned above. The test samples were 5 mm x 5 mm x 8 mm. In order to ensure that the stress was uniaxial and to reduce any lateral clamping effects<sup>3,36</sup>, two additional 6mm. long pieces of the same material were stacked on either side of the sample. The basic experimental set-up used in our laboratory for making these measurements has been described earlier.<sup>27</sup> A Monsanto tensometer is used in the compression mode and exerts a uniaxial stress on the sample assembly mounted between two insulators. A semi-circular base plate ensures that the stress is normal to the specimen. A Keithley 617 electrometer measures the current that is generated when a stress is applied to the specimen. The stress on the sample is determined by using the tensometer force head, whose output is read by a Keithley 199 digital multimeter and all data are fed into a computer. Under short circuit conditions,  $E = 0$ , and the electric displacement is given by the integral of the current with respect to time:

$$D_3 = d_{33}T_3 = \frac{1}{A} \int Idt \text{ so that } d_{33}(T_3) = \frac{\int Idt}{AT_3}, \quad (2)$$

where  $A$  is the electroded cross-sectional area of the sample. As discussed above, this will give the average value of  $d_{33}$  up to the stress level  $T_3$ . A differential  $d_{33}$  can be found from the slope of the curve giving the electric displacement as a function of the applied stress. Since the piezoelectric response takes a finite time, as will be discussed in the next section, and exhibits hysteresis, the values of the piezoelectric constant determined will depend on the ramping rate of the stress and on the previous stress level experienced by the sample.

The experimental set-up used to measure the dynamic response to a small AC stress superimposed on a DC pre-stress was based on the method described by Audigier et al.<sup>42</sup> A piezoelectric actuator and a piezoelectric dynamic force sensor were inserted between the sample and one of the insulators. The actuator was used to produce a small AC force and this force was detected by the force sensor. The electric displacement was determined as described above. The dielectric constant was measured at 1 kHz by using an HP 4284 LCR meter. The strain response to the AC stress was measured by a strain gauge and the elastic constant could thus be determined. All signals were measured by lock-in amplifiers to improve the signal to noise ratio. The dynamic values were measured with a 0.2 Hz AC stress with an amplitude of 1.5 MPa. The DC pre-stress was increased in steps of 10 MPa up to 160 MPa and the AC measurement was taken five minutes after each step increase in the pre-stress to give time for the full piezoelectric response to develop (see the following section).

Due to reasons of space only our dynamic measurements are discussed here. Figure 7 shows the experimental variation of the piezoelectric constant  $d_{33}$ , the elastic constant  $s_{33}^E$ , the dielectric constant  $\epsilon_{33}^T$  and the electromechanical coupling coefficient  $k_{33}$ , all as a function of the pre-stress for the hard EC-69 and the soft EC-65 PZT ceramics. When a stress is applied to the hard EC-69 ceramic, domain switching can lead to the production of new non-180° domain walls.<sup>43,44</sup> Also, the stress can cause de-ageing (de-pinning of domain walls) and both effects lead to an increase in  $d_{33}$  as seen in Fig. 7. This increase in the extrinsic contribution also causes the dielectric constant and the loss to increase, as observed earlier<sup>36,45</sup> and shown in Fig. 7. As the stress is further increased

the domain walls become progressively clamped by the stress and causes a decrease in the  $d_{33}$ . The figure also shows that when the stress is released the value of  $d_{33}$  recovers and indeed after a full stress cycle, the EC-69 ceramic shows a net increase in  $d_{33}$ . This confirms that there has been no depoling and the decrease in  $d_{33}$  under high stress is due to stress-induced clamping of domain walls. Just like EC-69, the soft EC-65 also shows an initial increase in  $d_{33}$  as the pre-stress is increased but the  $d_{33}$  begins to decrease at a fairly low stress level and there is little recovery of the  $d_{33}$  when the stress is released. It is clear that in this case the stress has caused significant depoling. This is the dominant effect at high stress, although a small recovery of  $d_{33}$  when the stress is being reduced suggests that some reversible stress-induced clamping of domain walls has also occurred. But it is clearly stress-induced de-poling that causes the dramatic reduction in  $d_{33}$  in EC-65 ceramic after a stress cycle. The significant drop in  $s_{33}^E$  after a full cycle is further evidence of the depoling of the specimen. On the other hand EC-69 shows little change in  $s_{33}^E$  but it shows a strong increase in its dielectric constant  $\epsilon_{33}^T$  that is normally an indication of de-ageing in the material.<sup>36</sup> Our measurements of the average and differential values of  $d_{33}$  as a function of stress have been described elsewhere.<sup>27</sup>

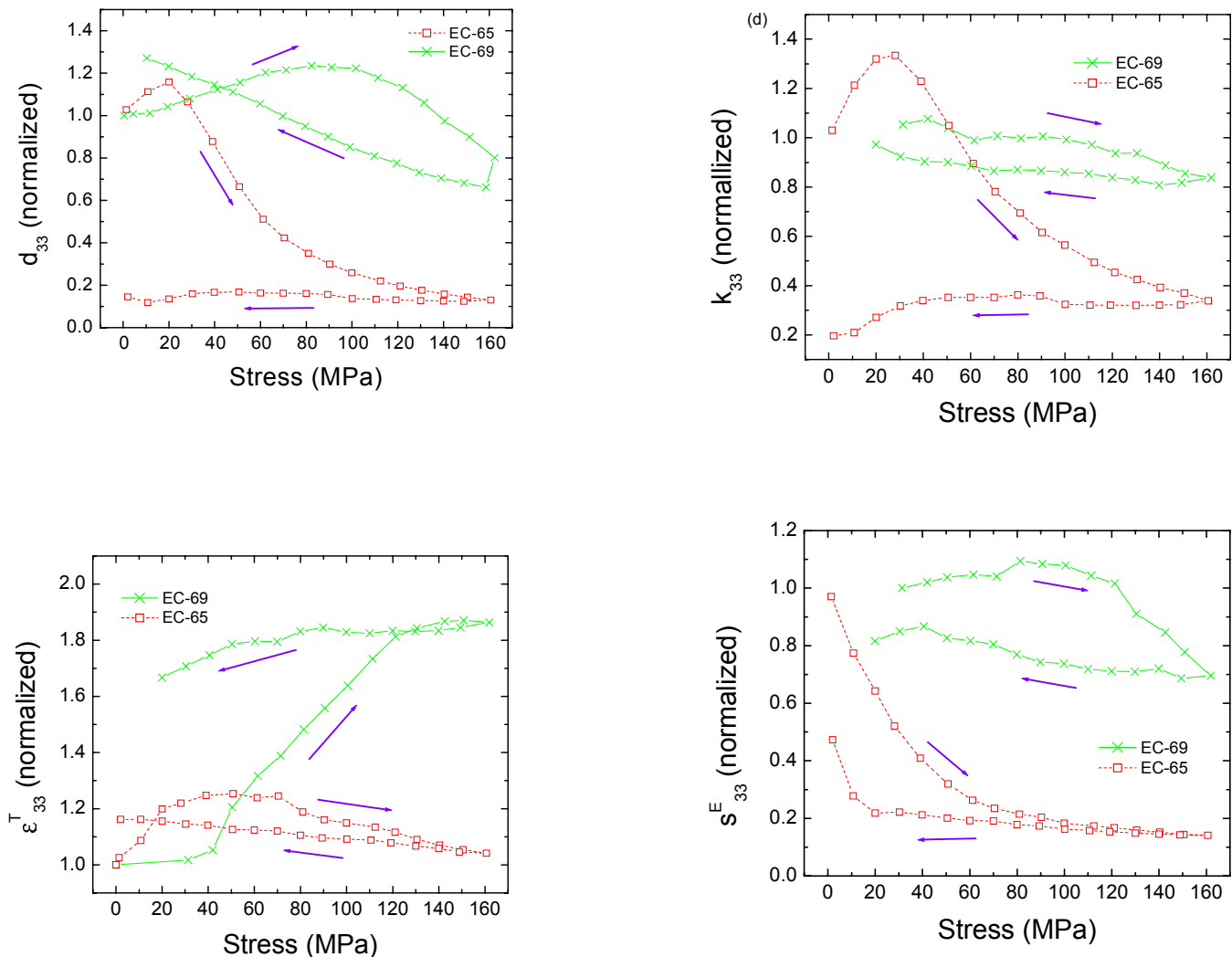


Figure 7: The stress dependence of the electromechanical properties of EC-69 and EC-65 PZT ceramics.

## Time Dependence of the Piezoelectric Response and Activation Energies of PZT Ceramics

As far back as 1959 it had been reported<sup>46</sup> that the piezoelectric response of a material was dependent on the rate of application of the electric field. Using an experimental method similar to that described in the previous section, we have investigated the time dependence of the piezoelectric response of PZT ceramics by applying a delta function stress step and measuring the polarisation produced by the piezoelectric response as a function of time. As we have reported earlier<sup>47</sup>, the piezoelectric response to the delta function stress step is made up of two parts: a fast response that corresponds to the intrinsic, 180° domain changes, and a slow increase that corresponds to the extrinsic, non-180° domain changes. The extrinsic contribution continues to increase several hundred seconds after the application of the step stress. A plot of the extrinsic polarisation response as a function of the logarithm of time yields a straight line whose slope,  $m$ , is found to be a function of temperature,  $T$ . This suggests that the domain wall motions that contribute to the extrinsic response are thermally activated. Clearly a ceramic material would have a distribution of activation energies. Arrhenius plots of  $\ln(mT)$  vs.  $1/T$  have allowed us to determine the average activation energies of various PZT ceramics. Typical values of the average activation energies obtained are 0.29 eV for a Navy Type I PZT ceramic and 0.62 eV for a Navy Type III PZT ceramic.<sup>47</sup> The time dependence of the piezoelectric response is responsible for the frequency dependence of the piezoelectric constant. A DC measurement can allow the piezoelectric response to develop fully. However as the frequency increases, smaller numbers of domains can change in the time available and the piezoelectric constant decreases.

## Characterisation of the New, High Strain, PZN-PT Single Crystals

$\langle 001 \rangle$  oriented single crystals of the relaxor ferroelectric solid solution  $\text{Pb}(\text{Zn}_{1/3}\text{Nb}_{2/3})\text{O}_3\text{-PbTiO}_3$  (PZN-PT) are known to exhibit high piezoelectric constants ( $d_{33} > 2000$  pC/N), high electromechanical coupling ( $k_{33} > 0.9$ ) and electric-field-induced strains up to 1.7%<sup>48,49</sup> and are therefore very promising for transducer and actuator applications. The very high strain values of these crystals are partly due to an applied electric-field-induced rhombohedral to tetragonal hysteretic phase transition.<sup>49,50</sup> We have investigated the strain response of two compositions of these PZN-PT crystals with PT contents of 4.5% and 8%, designated respectively as PZN-4.5%PT and PZN-8%PT. The crystals were grown by TRS Ceramics Inc. using a flux method and the samples provided to us had the dimensions of 5 mm x 5 mm x 1 mm and sputtered gold electrodes had been applied to them.

In a first experiment the strains produced by the crystals in the poling direction were measured as a function of a 0.2 Hz unipolar electric field and of temperature. A differential variable reluctance transducer was used to measure the strains while the samples were immersed in silicon oil that could be heated from 25° C to 105° C. Figure 8 shows the strain response of the  $\langle 001 \rangle$  oriented PZN-8%PT crystals as a function of a unipolar electric field at various temperatures. At room temperatures the poled crystals are in a stable multi-domain rhombohedral state with  $\langle 111 \rangle$  polar directions, called engineered domain configuration<sup>49</sup>, and little hysteresis is observed in the strain response. As the applied field is increased, hysteresis loops appear indicating the occurrence of an electric-field-induced phase transition from the rhombohedral to a tetragonal single domain state with a  $\langle 001 \rangle$  polar direction. The phase transition occurs at an electric field that decreases linearly with temperature<sup>51</sup> and at temperatures higher than 75°C PZN-8%PT crystals are already in the tetragonal phase without the need for any applied field. Similar results have been obtained for PZN-4.5%PT crystals.<sup>51</sup> The change in longitudinal strain,  $\Delta S_{33}$ , due to the phase transition is almost independent of temperature in the temperature range investigated, although the absolute strain value and the phase transition fields decrease as the temperature increases. We have found  $\Delta S_{33} \sim 0.4\%$  for the PZN-8%PT crystals in agreement with values obtained by Viehland<sup>52</sup> from bipolar field measurements. Figure 9 shows the temperature dependence of the piezoelectric constant  $d_{33}$  in the

rhombohedral phase and in the field-induced tetragonal phase of PZN-4.5%PT, as calculated from our direct strain measurements. In the rhombohedral phase,  $d_{33}$  increases with temperature in both crystals<sup>51</sup> and in the case of PZN-4.5%PT, the rate of increase itself increases significantly as the temperature rises above 60° C as shown in Fig.9. In the tetragonal phase the  $d_{33}$  does not change very significantly as a function of temperature.

Given that the rhombohedral phase provides the greater strain, the strain response of this phase has been further investigated as a function of AC applied fields and also as a function of DC bias fields. In this case the strains were measured directly with the Zygo laser Doppler interferometer that has been mentioned earlier and the  $d_{33}$  coefficient was derived from the strain measurements. Figure 10 shows the variation of the  $d_{33}$  of the two types of crystal as a function of applied field. At low applied fields the strain is non-hysteretic and varies linearly with electric field. As the electric field is increased beyond a threshold value  $E_t$ , hysteresis appears and the slope of the strain curve increases. This non-linear behaviour appears to be related to domain wall motion, as is the case in piezoelectric ceramics<sup>53</sup>, and the hysteresis is an indication of losses due to domain wall motions.  $E_t$  has been defined as the field at which  $\Delta d_{33}/d_{33}$  begins to exceed 2.5%, as was done by Li et al.<sup>53</sup> The  $E_t$  values obtained, 1.58 kV/cm for PZN-8%PT and 1.33 kV/cm for PZN-4.5%PT, were much higher than for soft PZT ceramics<sup>53</sup>, which indicates the existence of a stable domain configuration in the single crystals. PZN-8%PT shows greater non-linearity than PZN-4.5%PT and this is likely due to the fact that PZN-8%PT is closer to the morphotropic phase boundary (MPB)<sup>48</sup> so that domain walls move more easily and more significantly in response to the external field. It is also possible that

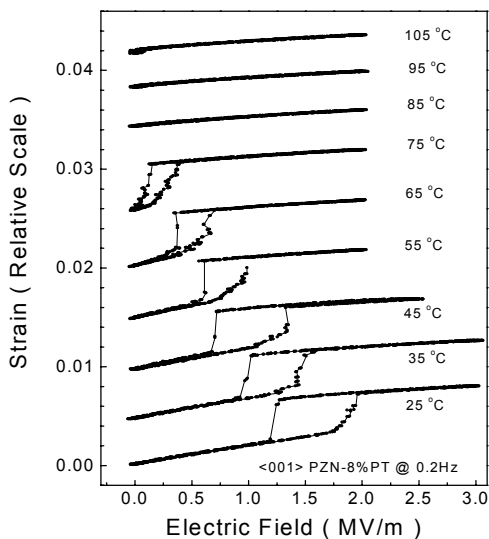


Figure 8: Unipolar electric field dependence of the strain response of PZN-8%PT single crystals at various temperatures.

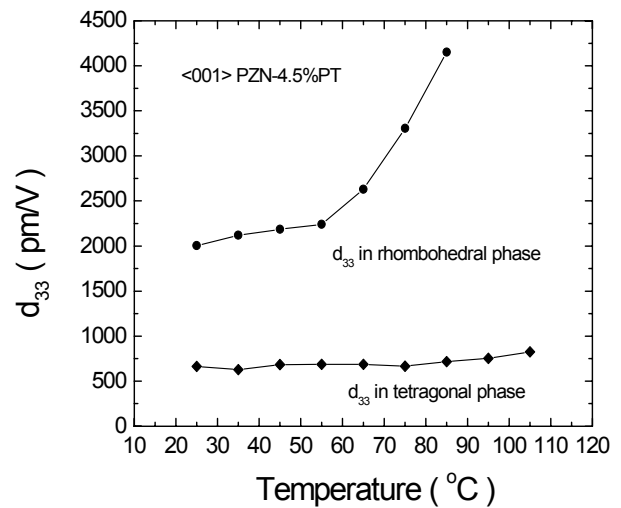


Figure 9: Temperature dependence of  $d_{33}$  in the rhombohedral phase and the tetragonal phase respectively in PZN-4.5%PT single crystals.

a newly discovered phase<sup>54</sup> around the MPB may also play an important role in the non-linear behaviour of the PZN-8%PT crystals. The dielectric constant of the crystals, as determined from polarisation measurements varies as a function of the AC field in a manner similar to the variation of  $d_{33}$ .<sup>55</sup> Figure 10 shows that the  $d_{33}$  measured with increasing fields is somewhat greater than the values found when the field is being decreased. This clearly indicates that irreversible domain motions have occurred and that the crystals are partially depoled even though the maximum field applied may be lower than the coercive fields of the crystals. The possibility of depoling severely limits the high power performance of the piezocrystals. We have investigated the possibility of using

a DC bias to stabilise the domain configuration and prevent the depoling caused by the application of large AC fields. Figure 11 shows the  $d_{33}$  coefficients of the two types of crystals, calculated from the strain responses, as a function of DC bias field. Clearly the region of linear response increases with

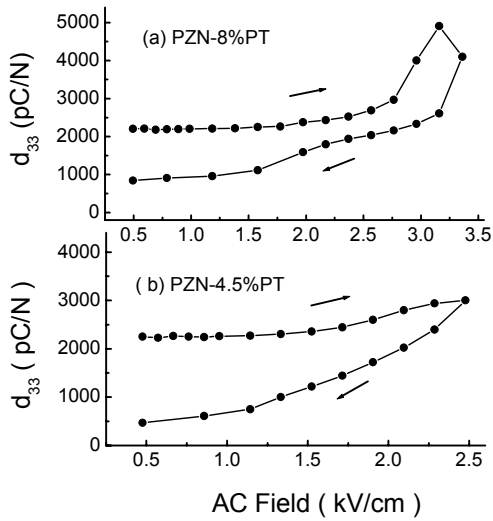


Figure 10: AC field dependence of the piezoelectric  $d_{33}$  for (a) PZN-8%PT and (b) PZN-4.5%PT, first with increasing field and then with decreasing field.

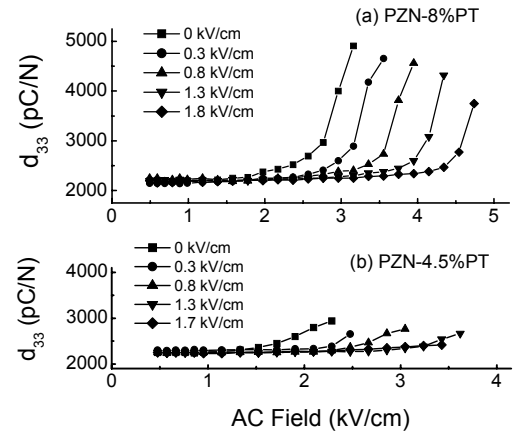


Figure 11: Effective piezoelectric coefficient  $d_{33}$  of (a) PZN-8%PT and (b) PZN-4.5%PT crystals, as a function of a 1 Hz electric field under various DC bias fields. The bias fields increase from left to right.

DC bias and Fig. 12 shows that the  $E_t$  increases linearly with DC bias. Our measurements clearly show that a positive DC bias can effectively stabilise the domain configuration in PZN-PT crystals and enhance the field interval over which their piezoelectric response is linear without significantly reducing the piezoelectric response of the crystal as happens in the case of piezoelectric ceramics.<sup>53</sup> Although the PZN-PT piezocrystals poled along the  $\langle 001 \rangle$  direction have large values of the longitudinal piezoelectric constant  $d_{33}$ , they have relatively poor shear strains with  $d_{15} \sim 140$  pC/N<sup>56</sup>. But Zhang et al<sup>57</sup> have reported that PZN-PT crystals poled along the  $\langle 111 \rangle$  direction show large shear strains but the values obtained by them, using resonance measurements, depended on approximate calculations since the elastic compliances required for a proper calculation were not available. Our Zygo laser Doppler interferometer system has been used to directly measure the shear strains in these materials for a 1 Hz AC excitation. From these strain measurements we have the following, very high, values of the piezoelectric shear coefficient:  $d_{15} \sim 5500$  pC/N for the PZN-4.5%PT crystal and  $d_{15} \sim 7500$  pC/N for the PZN-8%PT crystal. The effects of DC bias field and AC frequency on the shear piezoelectric coefficient of  $\langle 111 \rangle$  oriented PZN-PT crystals have also been studied. Figure 13 shows that the  $d_{15}$  coefficient decreased as the DC bias field increased. The  $d_{15}$  was also found to decrease as the AC frequency increased but the frequency dependence itself decreased as the DC bias was increased. These observations suggested that an increasing DC bias caused the crystal to approach a single domain state. Further details of our observations have been published elsewhere.<sup>58</sup>

## Conclusion

This paper has presented experimental observations to show that, except when very small excitation signals are applied, the piezoelectric, dielectric and elastic responses of a piezoelectric ceramic are essentially non-linear. The material constants have to be expressed as complex coefficients in order to take account of all the losses in the material and they have also been shown to change as a

function of temperature and frequency. The high strain PZN-PT single crystals have also been found to have non-linear properties. It is clear that, from the point of view of an applications/design engineer, it would be appropriate to have the material characterised under the same conditions as the material would be exposed to during the application. For reasons of space, we have only summarised the work carried out in our laboratory. A more general survey of some of the non-linear properties has been given by Gonnard<sup>59</sup> and by Damjanovic and Robert.<sup>60</sup>

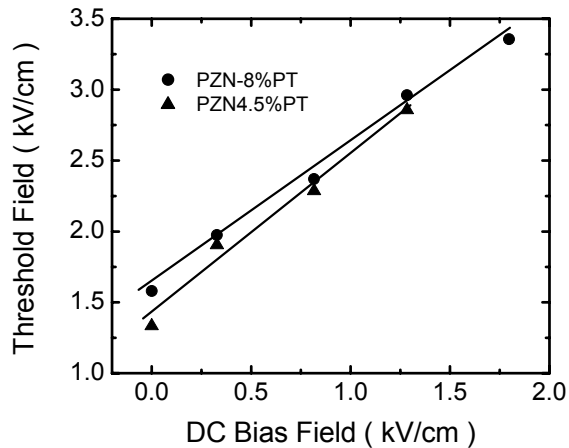


Figure 12: Threshold AC fields for the onset of non-linearity in PZN-8%PT and PZN-4.5%PT crystals as a function of DC bias.

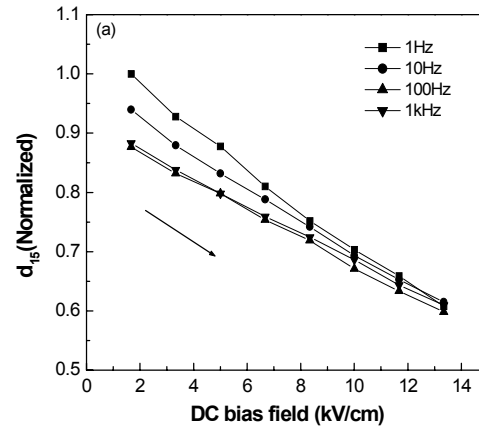


Figure 13: DC bias field dependence of  $d_{15}$  for  $\langle 111 \rangle$  oriented PZN-8%PT single crystals at four different frequencies (1 Hz, 10 Hz, 100 Hz, and 1 kHz) as DC bias is increased.

## Acknowledgements

The work reported here has been carried out with the help of my colleagues, amongst whom the following have made major contributions: Dr. Harvey Wiederick, who helped me to start our laboratory, Dr. Stewart Sherrit, who was successively, a graduate student and a research associate, Dr. Guomao Yang, Dr. Wei Ren and Mr. Shi-Fang Liu, who are all research associates and Major Tony Masys, who was a graduate student. Major funding for our laboratory has been provided, at various stages, by the Department of National Defence, Canada and by the Office of Naval Research, USA.

## References

- <sup>1</sup> A.F. Devonshire, *Phil. Mag. Supp.*, **3**, 85 (1952).
- <sup>2</sup> W.P. Mason, *Physical Acoustics and the Properties of Solids*, D. Van Nostrand Co. Inc. (Princeton, New Jersey) (1958).
- <sup>3</sup> Q.M. Zhang, J. Zhao, K. Uchino and J. Zheng, *J. Mater. Res.*, **12**, 226 (1997).
- <sup>4</sup> IEEE Standard on Piezoelectricity (1987), ANSI/IEEE Standard 176-1987.
- <sup>5</sup> PZFlex, from Flex Support, Weidlinger Associates, Inc., 4410 El Camino Real, Suite 110, Los Altos, CA 94022, USA, see <http://www.wai.com/AppliedScience/Software/Pzflex/index-pz.html>.
- <sup>6</sup> D.A. Berlincourt, D.R. Curran and H. Jaffe, *Physical Acoustics I Part A*, Chapter 3, pp.169-270, Academic Press: Editor W.P. Mason (1964).
- <sup>7</sup> A.H. Meitzler, H.M. O'Bryan and H.F. Tiersten, *IEEE Trans. on Sonics and Ultrasonics*, **SU-20**, 233 (1973).
- <sup>8</sup> R. Holland, *IEEE Trans. on Sonics and Ultrasonics*, **SU-14**, 18 (1967).
- <sup>9</sup> S. Sherrit, in *Electroactive Polymer (EAP) Actuators as Artificial Muscles: Reality, Potential and Challenges*, Ed.: Y. Bar-Cohen, SPIE Press, Bellingham, WA 98227-0010, USA (2001), Chapter 15.

- <sup>10</sup> R. Holland and E.P. Eernisse, *IEEE Trans. on Sonics and Ultrasonics*, SU-16, 173 (1969).
- <sup>11</sup> H. Ohigashi, T. Itoh, K. Kimura, T. Nakanishi and M. Suzuki, *Jap. J. Appl. Phys.*, 27, 354 (1988).
- <sup>12</sup> T. Tsurumi, T. Ichihara, K. Asaga and M. Daimon, *J. Amer. Cer. Soc.*, 73(5), 1330 (1990).
- <sup>13</sup> J.G. Smits, *IEEE Trans. on Sonics and Ultrasonics*, SU-23, 393 (1976)
- <sup>14</sup> S. Sherrit, H.D. Wiederick and B.K. Mukherjee, *Ferroelectrics*, 134, 111 (1992).
- <sup>15</sup> S. Sherrit, N. Gauthier, H. D. Wiederick and B. K. Mukherjee, *Ferroelectrics*, 119, 17 (1991).
- <sup>16</sup> C. Alemany, A.M. Gonzalez, L. Pardo, B. Jimenez, F. Carmona and J. Mendiola, *J. Phys. D: Appl. Phys.*, 28, 945 (1995).
- <sup>17</sup> B.K. Mukherjee and S. Sherrit, Proc. of the Fifth Int. Congress on Sound and Vibration, Vol.1, 385 (1997), The International Institute of Acoustics and Vibration, Dept. of Mech. Eng., Auburn University, AL 36849-5341, USA.
- <sup>18</sup> K.W. Kwok, H.L.W. Chan and C.L. Choy, *IEEE Trans. on Ultrasonics, Ferroelectrics, and Frequency Control*, 44, 733 (1997).
- <sup>19</sup> L. Pardo, this volume.
- <sup>20</sup> PRAP (Piezoelectric Resonance Analysis Programme) software available from TASI Technical Software Inc. See [www.tasitechnical.com](http://www.tasitechnical.com)
- <sup>21</sup> S. Sherrit and B.K. Mukherjee, Proc. of 1998 IEEE International Ultrasonics Symposium, IEEE, Piscataway, NJ (1998), 633 (1998).
- <sup>22</sup> S. Sherrit, H.D. Wiederick and B.K. Mukherjee, Medical Imaging1997: Ultrasonic Transducer Engineering (SPIE Proceedings Volume 3037), 158 (1997). SPIE Press, Bellingham, WA., USA.
- <sup>23</sup> S. Sherrit, J.E. Haysom, H.D. Wiederick, B.K. Mukherjee and M. Sayer, Proc. of the Tenth Int. Symp. on the Applications of Ferroelectrics, ISAF'96, 959 (1996). IEEE, Piscataway, N.J., USA.
- <sup>24</sup> S. Sherrit, H.D. Wiederick, B.K. Mukherjee and M. Sayer, *J. Phys.D: Appl. Phys.*, 30, 2354 (1997).
- <sup>25</sup> S. Sherrit, H.D. Wiederick and B.K. Mukherjee, Proc. of 1997 IEEE Ultrasonics Symposium, IEEE, Piscataway, NJ (1997), Vol.2, 931 (1997).
- <sup>26</sup> To be published.
- <sup>27</sup> G. Yang, S-F. Liu, W. Ren and B.K. Mukherjee, Smart Structures and Materials 2000: Smart Materials Technologies (SPIE Proceedings Volume 3992), 103 (2000). SPIE Press, Bellingham, WA., USA.
- <sup>28</sup> Q. M. Zhang, W.Y. Pan, S.J. Jang and L.E. Cross, *J. Appl. Phys.* 64, 6445 (1988).
- <sup>29</sup> S. Sherrit, H.D. Wiederick, B.K. Mukherjee and M. Sayer, Smart Structures and Materials 1997: Smart Materials Technologies (SPIE Proceedings Volume 3040), 99 (1997). SPIE Press, Bellingham, WA., USA.
- <sup>30</sup> H.D. Wiederick, S. Sherrit, R.B. Stimpson and B.K. Mukherjee, *Ferroelectrics*, 186, 25 (1996).
- <sup>31</sup> K.M. Rittenmyer and P.S. Dubbelday, *J. Acoust. Soc. Am.*, 91, 2254 (1992).
- <sup>32</sup> Zygo Corp., Laurel Brook Rd., Middlefield, CT 06455-0448, USA.
- <sup>33</sup> A.J. Masys, W. Ren, G. Yang and B.K. Mukherjee, *J. Appl. Phys.*, 94, 1155 (2003).
- <sup>34</sup> Q.M. Zhang, W.Y. Pan and L.E. Cross, *J. Appl. Phys.*, 63, 2492 (1988).
- <sup>35</sup> Q.M. Zhang, H. Wang, N. Kim and L.E. Cross, *J. Appl. Phys.*, 75, 454 (1994).
- <sup>36</sup> Q.M. Zhang and J. Zhao, *IEEE Trans. on Ultrasonics, Ferroelectrics, and Frequency Control*, 46, 1518 (1999).
- <sup>37</sup> Y. Masuda and A. Baba, *Jpn. J. Appl. Phys.*, 24 (Suppl 3), 113 (1985).
- <sup>38</sup> A.G. Luchaninov, A.V. Shil'nikov, L.A. Shuvalov and V.A. Malyshev, *Ferroelectrics*, 145, 235 (1993).
- <sup>39</sup> H. Cao and A. Evans, *J. Amer. Cer. Soc.*, 76, 890 (1993).
- <sup>40</sup> S.C. Hwang, C.S. Lynch and R.M. McMeeking, *Acta Metall. Mater.*, 43, 2073 (1995).
- <sup>41</sup> D. Guyomar, D. Audigier and L. Eyraud, Proc. of the Eleventh Int. Symp. on the Applications of Ferroelectrics, ISAF'98, 307 (1998). IEEE, Piscataway, N.J., USA.
- <sup>42</sup> D.Audigier, C. Richard, C. Descamps, M. Troccaz and L. Eyraud, *Ferroelectrics*, 154, 219 (1994).
- <sup>43</sup> A. Schaufele and K.H. Hardtl, *J. Amer. Cer. Soc.*, 79, 2637 (1996).
- <sup>44</sup> C.S. Lynch, *Acta Mater.*, 44, 4137 (1996).
- <sup>45</sup> H.H.A. Krueger, *J. Acoust. Soc. Am.*, 42, 636 (1967).
- <sup>46</sup> D. Berlincourt and H.H.A. Krueger, *J. Appl. Phys.*, 30, 1804 (1959).
- <sup>47</sup> S. Sherrit, D.B. Van Nice, J.T. Graham, B.K. Mukherjee and H.D. Wiederick, Proc. of the Eighth Int. Symp. on the Applications of Ferroelectrics, ISAF'92, 1005 (1992). IEEE, Piscataway, N.J., USA.
- <sup>48</sup> J. Kuwata, K. Uchino and S. Nomura, *Ferroelectrics*, 37, 579 (1981).
- <sup>49</sup> S.E. Park and T.R. Shrout, *J. Appl. Phys.*, 82, 1804 (1997).

- <sup>50</sup> S-F. Liu, S.E. Park, T.R. Shrout and L.E. Cross, *J. Appl. Phys.*, 85, 2810 (1999).
- <sup>51</sup> W. Ren, S-F. Liu and B.K. Mukherjee, *Appl. Phys. Letts.*, 80, 3174 (2002).
- <sup>52</sup> D. Viehland, *J. Appl. Phys.*, 88, 4794 (2000).
- <sup>53</sup> S. Li, W. Cao and L.E. Cross, *J. Appl. Phys.*, 69, 7219 (1991).
- <sup>54</sup> B. Noheda, D.E. Cox, G. Shirane, S.E. Park, L.E. Cross and Z. Zhong, *Phys. Rev. Lett.*, 86, 3891 (2001).
- <sup>55</sup> W. Ren, S-F. Liu and B.K. Mukherjee, *Appl. Phys. Lett.*, 83, 5268 (2003).
- <sup>56</sup> J.H. Yin, B. Jing and W. Cao, *IEEE Trans. on Ultrasonics, Ferroelectrics, and Frequency Control*, 47, 285 (2000).
- <sup>57</sup> S.J. Zhang, L. Laurent, S-F. Liu, S. Rhee, C.A. Randall and T.R. Shrout, *Jpn. J. Appl. Phys.*, 41, L1099 (2002).
- <sup>58</sup> S-F. Liu, W. Ren, B.K. Mukherjee, S.J. Zhang, T.R. Shrout, P.W. Rehrig and W.S. Hackenberger, *Appl. Phys. Lett.*, 83, 2886 (2003).
- <sup>59</sup> P. Gonnard, in Piezoelectric Materials and Devices, Ed.: N. Setter, Ceramics Laboratory, EPFL Swiss Federal Institute of Technology, Lausanne 1015, Switzerland, Chapter 16, (2002).
- <sup>60</sup> D. Damjanovic and G. Robert, in Piezoelectric Materials and Devices, Ed.: N. Setter, Ceramics Laboratory, EPFL Swiss Federal Institute of Technology, Lausanne 1015, Switzerland, Chapter 17, (2002).